Fig 19 Rate of energy consumption versus speed for human walking and running on the level (0%), up hill (+5% gradient), and down hill (−5% gradient). (From Margaria 1938)

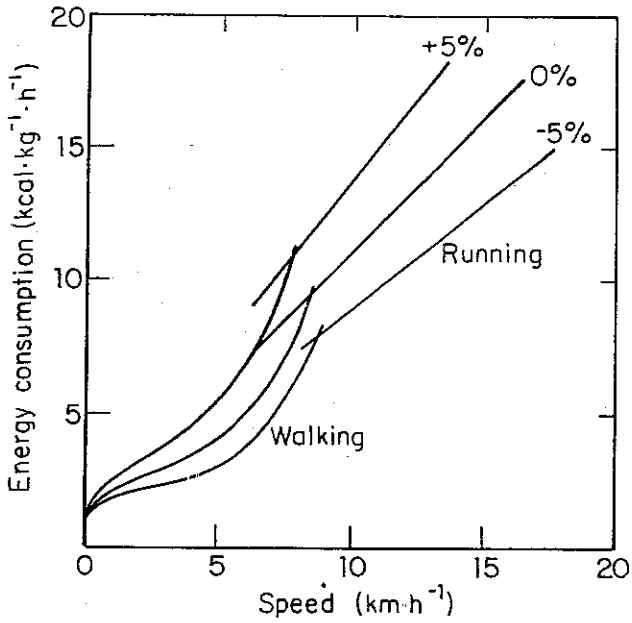

9. Up and Down Hills: Efficiency of Positive and Negative Work

Muscles are used to absorb mechanical energy as often as to create it. Physiologists have defined *negative work* as the work done by a muscle when it is developing an active force at the same time as it is being compelled to lengthen by some outside agency. The work *done* by the muscle under these circumstances is negative. When the muscle is allowed to shorten while developing force, it does *positive work*.

Using the fact that about 5 kcal of free energy is made available when 1 ml of oxygen is used in the aerobic combustion of food, a mechanical efficiency may be calculated for walking and running:

$$efficiency = \frac{mechanical\ work\ done}{chemical\ energy\ consumed} \qquad (3)$$

In this definition, the mechanical work done by the muscles in a step is estimated from the change in the average potential energy, given by the weight times the net change in height of the center of mass per step cycle. As a subject walks on level ground, the net change in height of the center of mass per step cycle is zero, so the calculated efficiency is zero. For walking on a gradient, however, there can be a nonzero efficiency because the center of mass is either steadily ascending or descending, leading to a steady rate of working against (or with) gravity.

9.1. Tilting Treadmill

Figure 19 shows the rate of energy consumption for a human subject walking on a tilting treadmill. Energy-consumption rate increases as a curvilinear function of speed for walking, but, as noted in Fig. 16, becomes a straight-line function of speed for running. At a given speed, the rate of energy consumption is increased as the treadmill belt is tipped up and decreased as it is tipped down.

As shown in Fig. 20, when energy consumption during walking is expressed per unit distance (obtained by dividing the rate by the speed), a series of curves emerges, each with a different minimum. At steep positive gradients, the optimal speed for minimizing energy consumption is in the range below 2 km/hr. As the gradient falls, the minimum broadens and shifts to higher speeds.

The lowering of energy cost as the treadmill belt is tipped down does not continue indefinitely, however, as is shown in Fig. 21. A minimum energy cost is reached at a gradient of about −10%. Negative gradients steeper than −10% are accompanied by increased energy costs for walking, even when the comparison is always made (as in Fig. 21) at the speed that minimizes the energy cost per unit distance.

9.2. Efficiency

This is where positive and negative work come in. The radial lines drawn through the zero point of Fig. 21 are lines of constant efficiency. Along any one of these lines, the energy cost per distance traveled increases directly with the weight-specific vertical work done per distance traveled, which is just the percent of incline of the ground. The lines corresponding to low efficiency lie above those corresponding to high efficiency, because walking up a given incline a given distance takes more energy at low efficiency. The points for

Fig 20 Energy consumption per unit distance in walking. For each gradient, a minimum occurs at a given speed. For the low and negative gradients, the minimum is very broad (From Margaria 1938)

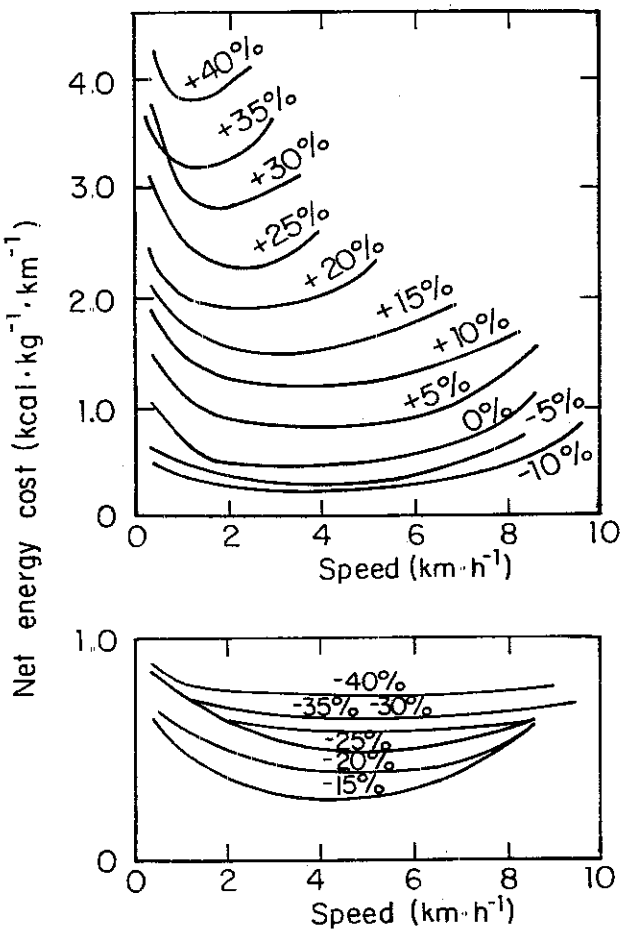

Fig 21 Energy cost per unit distance as a function of the inclination of the treadmill belt. For walking, the points represent speeds at or near the minima of Fig. 20. The radial lines from 0 show constant efficiencies, under the definition of (Eq. 3). (From Margaria et al. 1963)

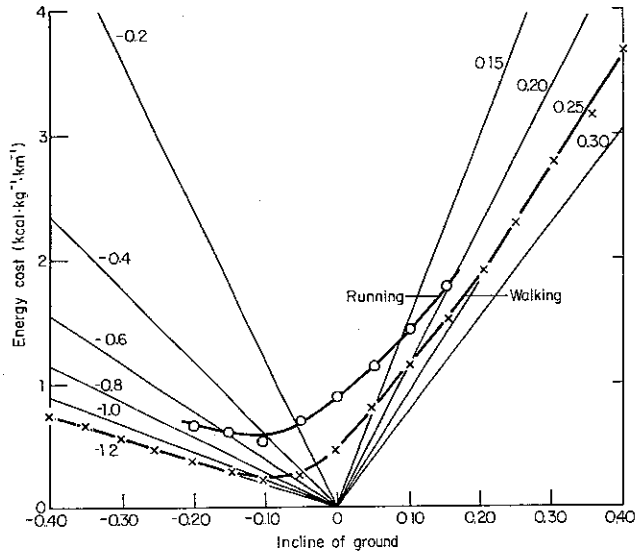

walking approach asymptotically the radial line representing 25% mechanical efficiency. At high positive gradients, walking becomes like climbing a ladder, and the muscles presumably are doing mostly positive work, since they develop substantial force only while shortening. Following this line of reasoning, Margaria (1976) has argued that the maximum efficiency with which a muscle may transfer chemical energy from the oxidation of food into mechanical work is about 25%.

A similar conclusion is reached for the region of high negative gradients, where the points for walking fall on the −1.20 efficiency line. Since the muscles of the subject are being used primarily for negative work in this region, Margaria concludes that the efficiency of muscles doing negative work is −120%. Note that a greater quantity of energy can be absorbed by a muscle as it is being stretched than can be released during shortening by the same muscle using the same number of moles of adenosine triphosphate (ATP).

As one might expect, the points on Fig. 21 representing running are vaguely asymptotic to the same lines as the points for walking. The running points, however, always lie above the walking points, because walking saves energy by storing it against gravity, as discussed earlier. The fact that the running points approach the +25% and −120% lines more slowly than the walking points can be interpreted as meaning that running up or down hill is still a mixture of positive and negative work, and remains so even at inclines that would have converted walking purely to one form or the other.

A conclusion to be drawn from the paragraphs above is that while animals walking or running up or down a steep enough hill are doing exclusively positive or negative work, the muscles of animals walking or running on level ground are doing both positive and negative work in each step. Additionally, elastic storage of energy in tendons, muscles, ligaments, and bones may be used, particularly during running, to change the kinetic energy of the center of mass as the animal rebounds from the ground. The changes in kinetic energy would have to be paid for by metabolic

Fig. 22. Animals running with weights on their backs. A. The time during which each foot was in contact with the ground was the same in a given animal at a given speed with and without weights. Each pattern shows the average of 10 strides, with bars to indicate the standard error (SE) of the mean. B. The rate of oxygen consumption increased by the same factor as the increase in gross weight when the animals carried loads. Each point represents the mean of a single running speed, including the data for several animals. The bars show ±2 SE. L = left, R = right, F = forefoot, H = hind foot. (From Taylor et al. 1980)

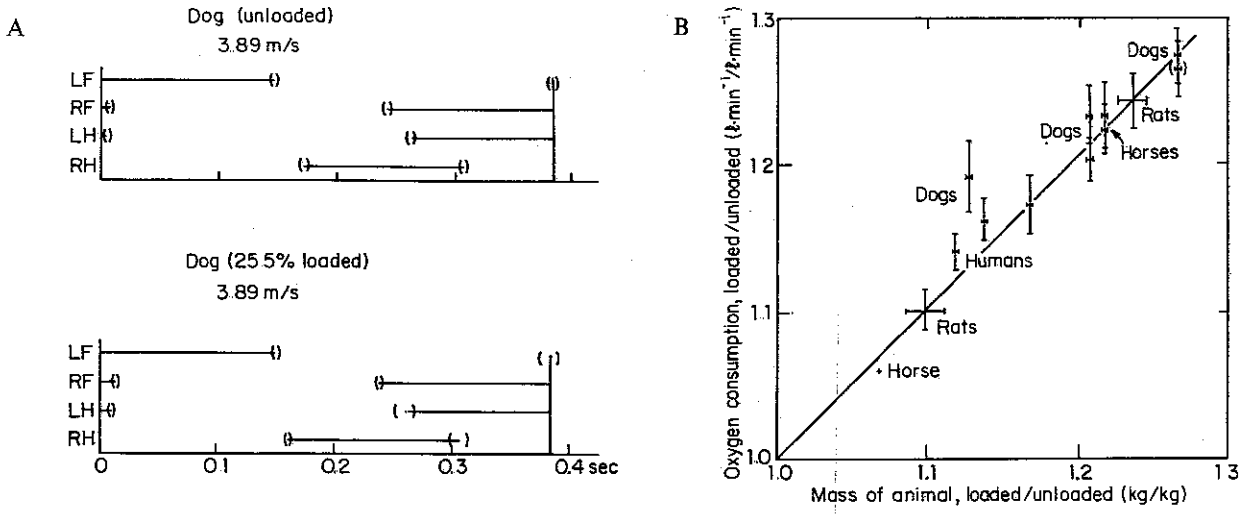

energy utilization if the elastic storage mechanisms were not available.

These considerations show that it is not realistic to expect to measure the rate at which mechanical work is done as the center of mass is lifted periodically during running and relate that figure to metabolic power. Even when proper care is taken to measure separately the positive and negative work done on the center of mass, the impossibility of calculating the amount of energy transiently stored in elastic forms makes the determination of muscle efficiency for level walking and running seem impractical.

There is also a commonsense objection. It is well known that isometric muscular activities require metabolic energy, but their mechanical efficiency is always zero, by the definition of (Eq. 3). A great deal of empirical evidence exists showing that the energy consumed as a muscle contracts under isometric constraints is proportional to the area under the curve of muscle force versus time, the so-called *tension-time integral* (Sandbert and Carlson 1966; Stainsby and Fales 1973; Kushmerick and Paul 1976). Mathematical models of ATP utilization by crossbridge attachment, force generation, and detachment would predict just exactly this, because the rate of isometric ATP splitting depends on the developed tension in such models (Huxley 1957; Eisenberg, Hill, and Chen 1980; Wood 1981).

10. Running with Weights

It is possible to show that the rate of oxygen consumption depends directly on muscle tension in running animals, as well as in isometric studies of isolated muscles. This was done by measuring the oxygen consumption of animals trained to run with weights on their backs.

Rats, dogs of various sizes, horses, and men were trained to run on a treadmill carrying weights in specially made packs. It was found, after the training period of one to three weeks, that the stride frequency was the same in a given animal at a particular speed, whether or not it was carrying weights on its back up to nearly 30% of body weight. The same was true of the time of contact of each foot (Fig. 22A) and the average upward vertical acceleration during the time the feet were on the ground, as measured by an accelerometer on the animal's back. Since none of these parameters changed whether the animal was loaded or unloaded at a particular speed, the kinematics of the center of mass were judged to be unaffected by load carrying.

If the acceleration of the center of mass at an arbitrary instant of the stride cycle was unaffected by the load, then, by Newton's law, the force in every major muscle involved in locomotion must have risen in direct proportion to the change in gross weight when

the load was added. A 10% increase in gross weight would lead to a 10% increase in instantaneous muscle force.

10.1 Oxygen Consumption and Load

The loaded/unloaded ratio of rates of oxygen consumption is shown in Fig. 22B. This ratio is seen to be directly related to the loaded/unloaded ratio of gross weights, so that a 10% increase in gross weight leads to a 10% increase in rate of oxygen consumption. Each point shows the mean of several animals running at a single speed. The speeds were such that the rats and horses trotted, the humans ran, and the dogs either trotted or galloped. Invariably, the loaded/unloaded ratio of oxygen consumption rates did not depend on the running speed, but only on the gross weight.

One of the conclusions is easy to draw. Since both muscle force and rate of oxygen consumption were increased by the same factor during load carrying, the rate of oxygen consumption must be proportional to muscle tension, all other things being the same. This is in agreement with the isometric studies on isolated muscles, which found that oxygen utilization depended on the tension-time integral.

Because of the way the load-carrying experiments were done, however, it is not possible to claim that they prove the tension-time integral is the *only* determinant of oxygen consumption. Since the vertical excursions of the center of mass were unchanged by load carrying, the rate of working against gravity increased by the same factor as the gross weight increase. Therefore, an interpretation based on an unchanging muscle efficiency and a weight-proportional increase in stored elastic energy would also be admitted by the results.

10.2 Carrying a Load Is Not Equivalent to Increasing Speed

A more profitable way of looking at oxygen utilization during running on a flat surface is to leave aside entirely the concept of muscle efficiency. We must be prepared to admit that as an animal runs faster, a great number of complicated things change. Both the speed of shortening and the peak force experienced by the muscles increase. Each one of these can be expected to increase ATP turnover rate, and hence oxygen utilization.

Furthermore, additional muscle fibers and even whole muscles are recruited as they are needed at higher speeds. For example, studies of the electrical activity of muscles in dogs show that a major muscle of the trunk, iliocostalis lumborum, is inactive in a walk and a trot but becomes active in a gallop (Taylor 1978).

11. Enhanced Gravity: Running in Circles

An experiment that has a great deal in common with load carrying is the effective enhancement of gravity obtained by running on a circular path. The centripetal acceleration v^2/R adds vectorially with the acceleration due to gravity to produce higher foot forces, just as increasing the body weight produces higher foot forces.

Figure 23 shows results of an experiment in which subjects were instructed to run as fast as possible along a circular path marked on a sod surface. All the subjects wore spiked shoes. A high-speed motion picture camera filmed the runs for later analysis. It was observed that both the stride frequency and the step length were virtually unaffected by the radius of the turn, while the time the runner's foot was in contact with the ground was almost doubled at the smallest radius (4 m). Since the step length (the distance the body moves forward during a ground contact period) was unaffected but contact time was increased, the runner's speed was markedly reduced on the sharp turns.

A simple theory may be proposed for understanding these experimental results. Suppose that a bipedal runner moves in a series of aerial phases and contact phases. During the aerial phase, the runner travels a distance $t_a v$ along a straight line over the ground, as shown in Fig. 23C. During the contact phase, we assume that the vertical projection of the runner's motion is a circular arc of radius R', which begins tangent to the straight line describing the aerial phase. In one half-stride, therefore, the direction of the runner's motion is changed through an angle $\Delta\theta$.

If the direction of the runner's motion changed at a

Fig 23. Running on a circular track. A subject ran at top speed around concentric circular tracks ruled on turf. A. Speed drops off sharply with decreasing radius. B. Stride time T is approximately constant, but ground-contact time t_c increases and aerial time t_a decreases at small radii. C. Diagrams used in explaining the theory. Solid lines show theoretical results. Points show mean and error bars due to film reading for several runs of a single subject. At the smaller radii, the subject's feet slipped somewhat, even though he was wearing spiked shoes. This effect is not taken into account in the theory, and may be one source of the lack of agreement between theory and experiment at low turn radii.

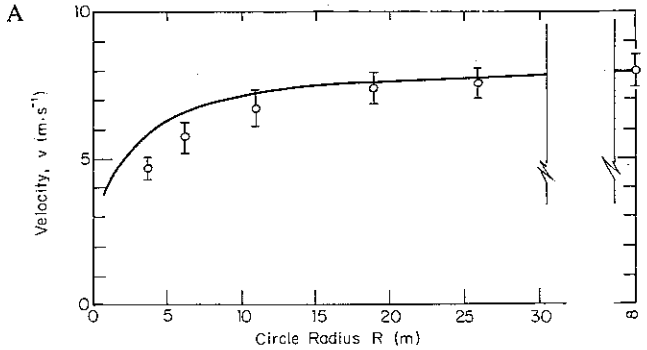

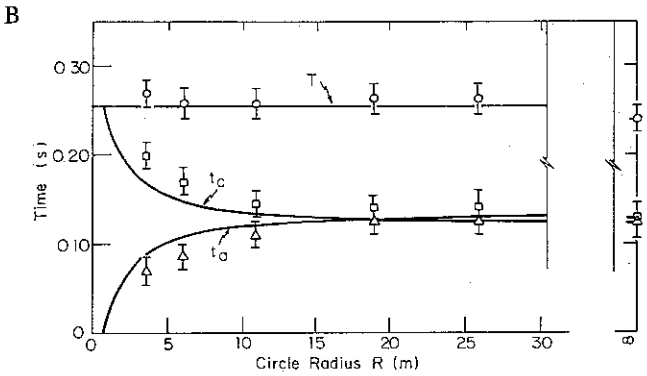

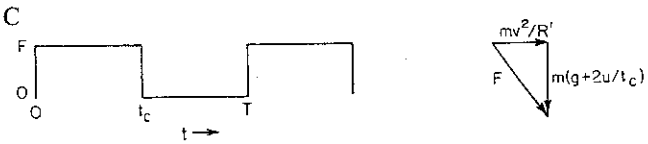

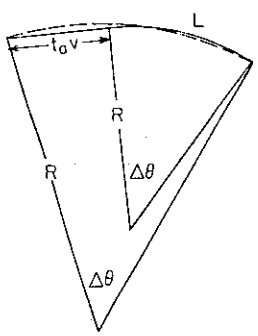

constant rate during the whole stride, that is, during the aerial phase as well as the contact phase, the vertical projection of the runner's motion would be a circular path of radius R. The relationship between R' and R is established by the fact that the angle $\Delta\theta$ is the same for both arcs. For small angles $\Delta\theta$, the arc length $R\Delta\theta$ is approximately given by

$$R\Delta\theta \simeq t_a v + L, \tag{4}$$

where t_a is the period of the airborne phase and L is the step length (the distance the body moves forward during one contact phase). We shall assume that the stride frequency and step length are independent of the turn radius.

Since

$$\Delta\theta = L/R', \tag{5}$$

$$R = \left(1 + \frac{t_a v}{L}\right) R'. \tag{6}$$

The radius R' may be found using the following argument. We begin by assuming (following the experimental evidence) that

$$T = \text{constant} \tag{7}$$

and

$$vt_c = L = \text{another constant}. \tag{8}$$

Here, $2T$ is the time for one complete stride, including two contact phases and two aerial phases. We assume that the foot force is a square wave of constant amplitude F and variable duration t_c. Then,

$$F = (mass) \times (acceleration) \tag{9}$$

and

$$F^2 = m^2\left[\left(\frac{v^2}{R'}\right)^2 + \left(g + \frac{2u}{t_c}\right)^2\right], \tag{10}$$

where u is the vertical velocity, which must be reversed upon landing. From the dynamics of the airborne phase,

$$2u = g(T - t_c) = g(T - L/v) \tag{11}$$

Substituting the above and rearranging,

$$\left(\frac{v^2}{R'}\right)^2 = \frac{F^2}{m^2} - [g + g(T - L/v)/(L/v)]^2 \tag{12}$$

and

$$\left(\frac{v^2}{R'}\right)^2 = \frac{F^2}{m^2} - g^2 \frac{v^2}{L^2} T^2 \tag{13}$$

When $R' \rightarrow \infty$, $v \rightarrow v_{max}$, so

$$\frac{F^2}{m^2} = \frac{g^2 v_{max}^2 T^2}{L^2} \tag{14}$$

Substituting (Eq. 14) into (Eq. 13),

$$\left(\frac{v^2}{R'}\right)^2 = \frac{g^2 T^2}{L^2}(v_{max}^2 - v^2) \tag{15}$$

and, therefore,

$$R'(v) = \frac{v^2}{g(T/L)(v_{max}^2 - v^2)^{1/2}} \tag{16}$$

Using the relation between R and R' obtained in (Eq. 6),

$$R(v) = \frac{v^2(1 + t_a v/L)}{g(T/L)(v_{max}^2 - v^2)^{1/2}} \tag{17}$$

This is the relation we have been seeking between the runner's speed and the radius R of the curved path the runner follows, on the average, between the straight aerial segments and the curved ground-contact segments. Following a convention suggested by Greene (1983), this relation may be given in a form in which dimensionless variables appear:

$$\frac{Rg}{v_{max}^2} = \frac{(v/v_{max})^2(1 + t_a v/L)}{(Tv_{max}/L)(1 - v^2/v_{max}^2)^{1/2}} \tag{18}$$

The theoretical results (including Eq. 17) are shown as solid lines in Fig. 23. As simple as this model is, it makes a fairly satisfactory prediction for the way in which ground-contact time, aerial time, and running speed change with turn radius. Note that the aerial phase is predicted to disappear entirely when the turn radius falls below about 1 m. This is not a practical point to check with running experiments, because under such circumstances the radius of the turn would be almost the same size as the step length. The prediction does serve to show, however, that running degenerates to walking (no aerial phase) when gravitational acceleration is sufficiently increased—as it would be, for example, on the larger planets.

This result fits well with the earlier discussion of walking under conditions of altered gravity. Following those arguments, we see that, since walking speed should increase under enhanced gravity and running speed should decrease, there comes a point when walking and running are the same thing. In this mode of progression, peculiar to movement on planets with high gravity, there is no aerial phase because the muscles are not strong enough to produce one. Nevertheless, a hypothetical human on a large planet will walk at a quite high speed in order to take advantage of the energy-exchange mechanisms of ballistic walking.

12. Utilizing Elastic Rebound: The Tuned Track

Running on a soft surface is more comfortable than running on a hard one. For training, runners prefer sod to concrete. In competition, however, it has generally been assumed by coaches and athletes that the hardest surface is the fastest.

In fact, this is not quite true. In what follows, it will be shown that there exists a particular set of mechanical properties for a running track that both lowers the potential for injury and slightly enhances speed.

12.1. A Model of the Leg

A conceptual model for the mechanical properties of the leg important in running is shown in Fig. 24. This model is based on both the intrinsic features of isolated muscle and the global features of muscle controlled by reflex networks and movement commands. The parallel spring and dashpot in Fig. 24 represent

Fig 24 Conceptual model of the leg used to predict a runner's performance on a compliant track Descending commands from the cortex, brain stem, and spinal centers (acting to crank the rack and pinion) are assumed to be separate from the mechanical properties of the muscles plus local reflexes (parallel spring and dashpot) (From McMahon and Greene 1979)

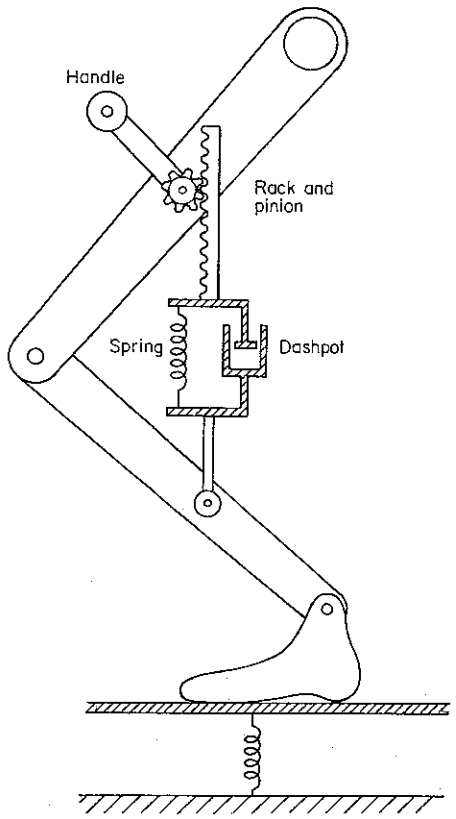

Fig 25 Foot-contact time versus track stiffness The solid line was calculated on the basis of the model shown in the inset, with the runner's damping ratio, $b/(2m^{1/2}k_m^{1/2})$, chosen as 0 55 Foot-contact time was computed for the model by calculating the half-period of oscillation of the runner's mass, m, as the track stiffness, k_t, changed Points show the results of many runners on both board and foam-pillow tracks Contact time, t_c, has been normalized by the contact time on a hard surface, t_0 The shaded region shows the range of track stiffness where the runner's speed should be enhanced most effectively Low values for t_c mean high running speed because speed $= L/t_c$, where L is the step length (From McMahon and Greene 1978)

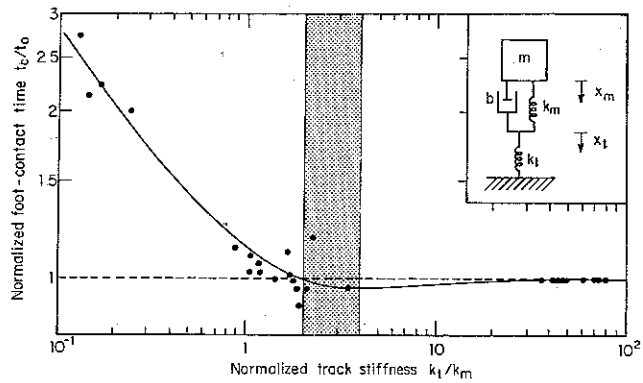

the "damped spring" character of the antigravity muscles of the leg working within the stretch-reflex loop

Reflexes, however, require some time to act The delay between a change in muscle load and the accompanying reflex change in electromyographic activity is found to be in the range of 80 ms for elbow flexion in humans (Crago, Houk, and Hasan 1976) and near 25 ms for soleus muscles in decerebrate cats (Nichols and Houk 1976) Melvill Jones and Watt (1971) have shown that approximately 102 ms elapses between otolith stimulation (by a sudden fall) and activation of the antigravity muscles in humans In running, the foot-contact period typically lasts 120 ms, so neither the vestibular reflexes nor the stretch reflexes have time to act in the first quarter of the stance phase For this reason, the spring and dashpot of Fig 24 represent the intrinsic mechanical properties of skeletal muscle in the first quarter or so of the foot-contact period; thereafter they represent the controlled, or reflex properties

The leg of Fig 24 would work in the following way Movement commands from the pattern generator in the spinal cord would crank the rack and pinion into the proper position for landing Then the rack and pinion would be locked, as far as vertical motions go, and the runner's rebound from the ground would be determined by the resonant motion of the body mass against the damped spring

12.2 Foot-Contact Time

The assumption that the contact time of the foot is equal to half the period of resonant vibration is, of course, an approximation In the inset of Fig 25, the springs have been shown attached Only that half-cycle of the motion for positive downward displacements of the runner (x_m) and the track (x_t) has any correspondence with reality When x_m is negative, the runner's foot actually would be separated from the track surface Although the permanent connection of the runner to the track is fictitious, it makes the mathematics convenient and corresponds approximately to the real situation during the contact portion of the step cycle

The solution of the differential equation describing the motion of the runner's mass is shown as a solid line in Fig 25 The equation itself is derived by

Fig. 26 Running on an experimental board track. Plywood boards are attached to 2 × 4 in. rails (underneath) to produce a very compliant running surface. The rails may be moved outward or inward to vary the compliance. A force plate under one of the panels of the track (not shown) records the vertical force. Electronic timing and high-speed motion picture film were also used. (From McMahon and Greene 1978.)

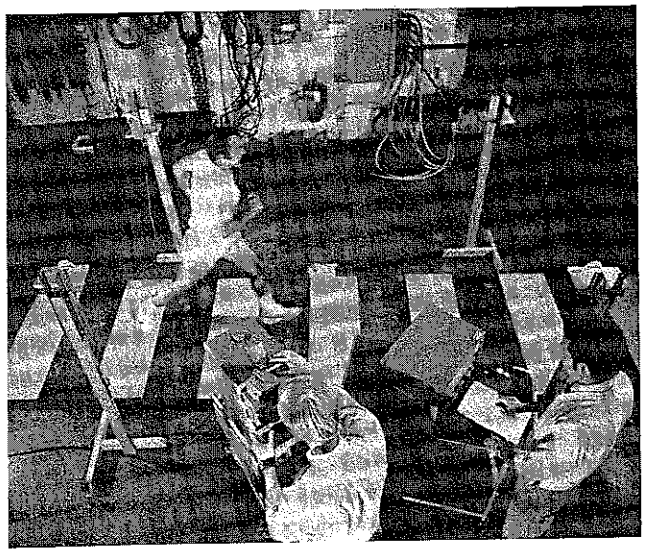

Fig. 27 Multiple-exposure photographs showing a subject running at top speed on a hard surface (top) and on a very compliant track made of foam pillows (bottom). (From McMahon and Greene 1978.)

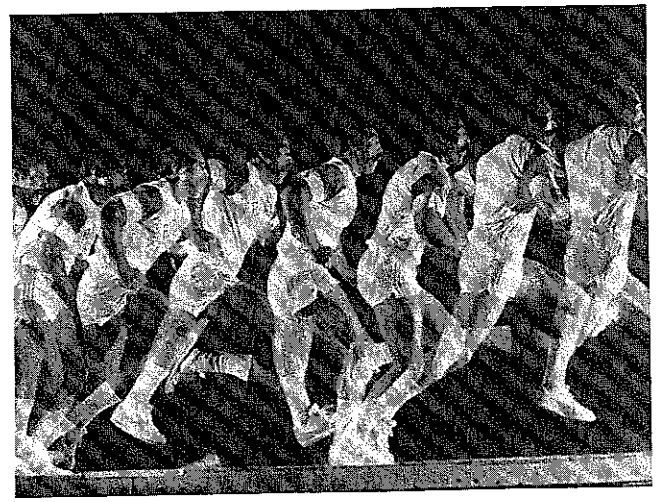

McMahon and Greene (1979). Foot-contact time t_c has been calculated from the half-period of ω_d, the damped resonant frequency, using $t_c = \pi/\omega_d$. The damping ratio $\xi = b/(2\sqrt{mk_m})$ has been assumed to be 0.55, because this value gives the best agreement between the theory and the experimental points.

The experimental points were obtained from running trials on a specially made board track (Fig. 26) and a very compliant track made from large foam-rubber pillows (Fig. 27). The stiffness of the board track could be adjusted by moving a set of 2 × 4 in. supporting rails outward or inward, thus increasing or decreasing the unsupported span of the plywood panels making up the top surface. Runners were told only to run as fast as possible alternately on one or the other of the experimental tracks and on a concrete surface. Their foot contact times were measured by high-speed photography and a force plate under one of the board-track panels.

As shown at the left of Fig. 25, foot-contact time is very much increased on the softest surfaces. This is really no surprise—anyone who has tried to run on a trampoline or a diving board knows that it takes longer to rebound from a soft, springy surface than from a hard one. The remarkable thing is that the theory predicts that foot contact time falls below its hard-surface value in the intermediate range of track stiffnesses, the shaded band at the center of the figure. This prediction is the key to the possibility of enhanced running speeds on tracks that are "tuned" within the range of spring stiffnesses shown by the shaded band, because running velocity is inversely proportional to ground-contact time.

12.3 Step Length

During the time the runner's foot touches the track, speed is determined by step length divided by contact time. The influence of track stiffness on step length is therefore an important matter and deserves further consideration.

Fig. 28. Stick figures showing a subject running on a hard surface (top) and on foam pillows (bottom). The angles mark the runner's right hip, ear, shoulder, elbow, wrist, and both knees, ankles, and shoe tips. The framing speed of the camera was 59 frames/second in each case. Only those frames where the foot touches the ground are drawn. The broken line (bottom) indicates the mean deflection of the pillows over a step cycle. Note that contact time is increased on the soft surface (there are more frames drawn), but step length is also increased (the hip moves a greater distance forward during foot contact). (From McMahon and Greene 1979.)

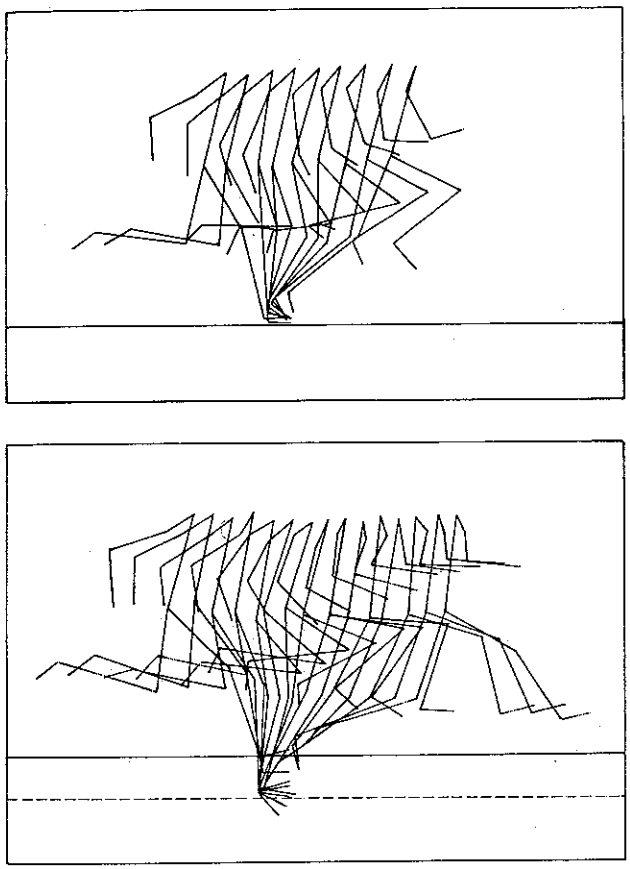

Fig. 29. Contact time t_c versus inverse running speed $1/v$ for one subject. The straight lines through the origin demonstrate that an individual's step length is constant, independent of running speed, on a particular surface. As shown in Fig. 27, step length is greater on the pillow track than on the hard surface. The error bars show uncertainty due to film reading. (From McMahon and Greene 1979.)

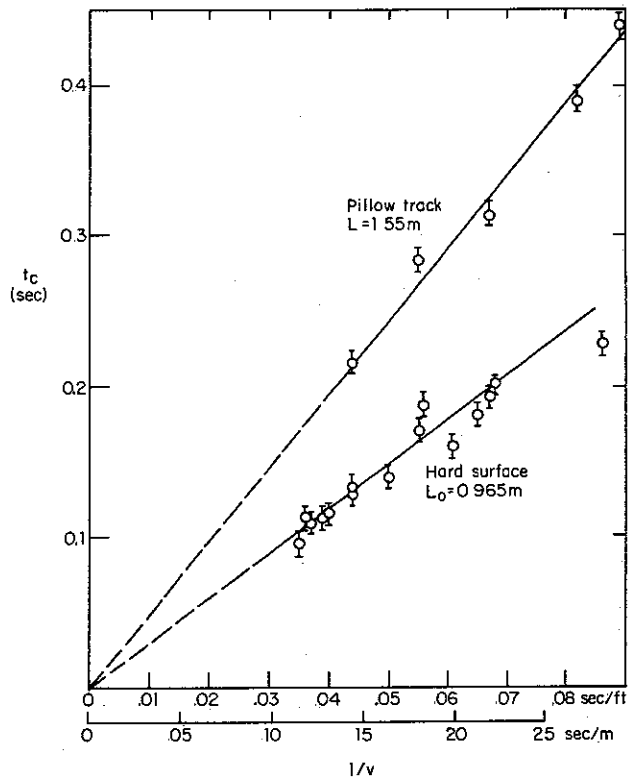

In Figs. 27 and 28, a comparison is shown between a running step on a hard surface and one on foam pillows. In Fig. 28, stick figures are shown for only those frames of the motion picture film when the foot touched the track surface. There are more stick figures in the bottom picture than in the top because foot-contact time was greater on the pillows than on the hard surface. The hip moves a greater horizontal distance in the bottom picture because step length is greater on the pillows than on the hard surface.

The circle-running experiments of Section 11 showed that step length did not change appreciably as track radius varied. In this section, we have seen that step length is also about the same at a variety of running speeds on a given surface, perhaps because of physiological limitations on hip flexion and hip and ankle extension. In Fig. 29, the ground-contact time t_c is plotted against the inverse of the running speed, $1/v$, for an individual subject running alternately on the concrete surface and the pillow track. The straight lines show $t_c = L/v$, where the step length L is a constant chosen to fit through the points. There is one constant, $L = 1.55$ m, which works well for the pillow-track points, and another, $L_0 = 0.965$ m, which fits the hard-surface points. The observation that step length is approximately independent of running speed (on a hard surface) was also made by Cavagna, Thys, and Zamboni (1976).

To see why step length should change with track stiffness, look closely at the stick figures in Fig. 28. A basic assumption in the argument to follow is that the trajectory of the trunk, and therefore of the hip, moves on a straight line parallel to the ground. In fact, this is not quite true, but Figs. 27 and 28 show that the verti-

Fig 30 Schematic illustration showing why step length is greater on a compliant surface (B) than on a hard one (A). On a soft track, the stance foot descends an average distance δ below the undeflected surface The broken lines show the swing leg moving forward, the solid lines slow successive positions of the stance leg as it moves back (From McMahon and Greene 1979.)

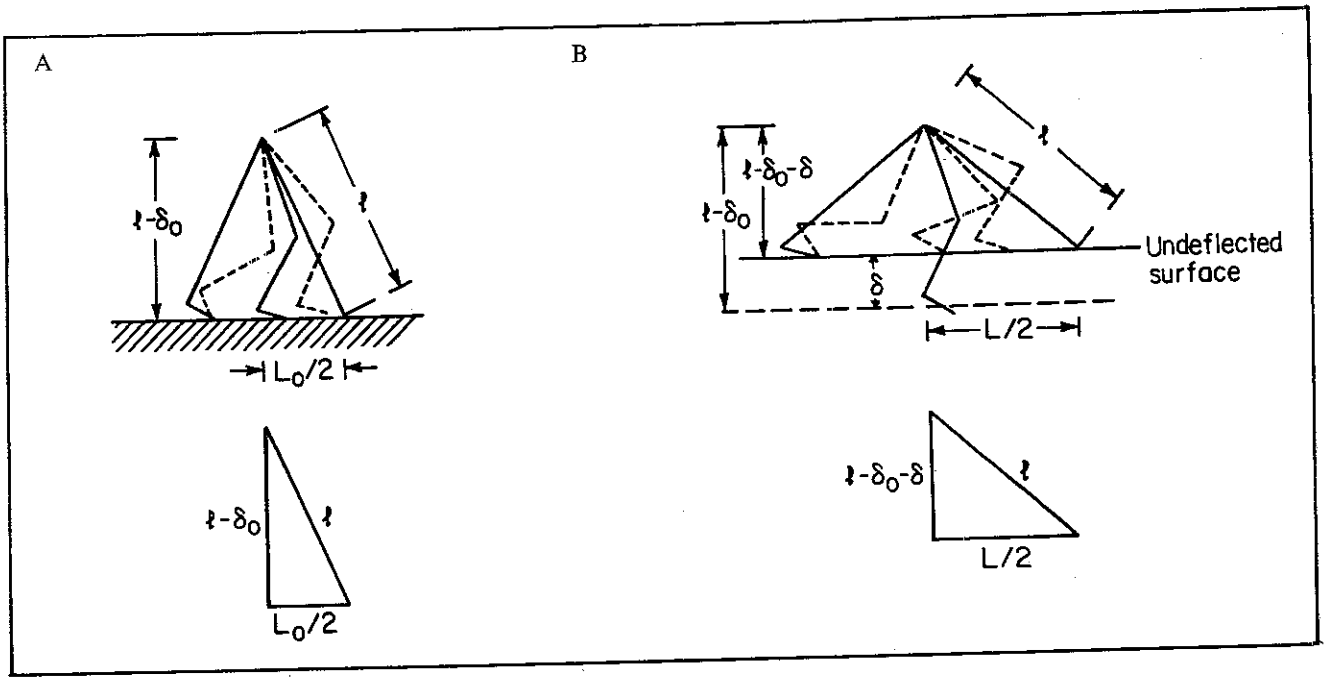

cal motion of the hip is about the same on the hard and soft surfaces, perhaps because the time the body is off the ground is so small in each case that not much vertical falling is possible.

When the runner moves over the pillows, as shown at the bottom of Fig. 28, the stance foot sinks into the foam rubber, but the swing foot always remains above the undeflected pillow surface. The extended leg encounters the pillow surface in a position when hip flexion is greater than is the case for running on a hard surface. This makes step length on the pillow surface relatively greater.

It is this observation which underlies the geometric model for calculating the dependence of step length on track stiffness shown in (Fig. 30). The leg, length ℓ, is shown with the knee fully extended at the moment of contact with each surface.

At midstance, the hip-to-ground distance is only $\ell - \delta_0$, where the shortening δ_0 is assumed to be a constant length, independent of running speed, cranked in by the "rack-and-pinion" central nervous system motor centers for the purpose of maintaining the body on a level trajectory. This assumption effectively ignores surface-dependent changes in the maximum compression of the damped spring, by comparison with the large displacement produced by the rack-and-pinion "postural controllers." Since $\delta_0 =$ 9.6 cm for the subject used to construct Fig. 28, while the maximum variation in compression of the damped spring on the hard and soft surfaces would be <0.56 cm (i.e., $<6\%$ of δ_0), the assumption seems justified.

Applying the Pythagorean theorem to the triangle in Fig. 30B,

$$L = 2\sqrt{\ell^2 - (\ell - \delta_0 - \delta)^2}, \tag{19}$$

where δ is the deflection of the pillow surface. Interpreted strictly, δ should refer to the peak deflection of the track surface at midstep, but, as an approximation, we let it be the mean deflection over the entire stride cycle. If the subject were not running at all, but were merely standing quietly on the pillows, he or she would be standing in a well of depth $\delta = mg/k_t$, where k_t is the spring constant for the pillows.

The constant δ_0 may be written in terms of the step length on the hard surface, L_0:

$$\delta_0 = \ell - \sqrt{\ell^2 - L_0^2/4}. \tag{20}$$

Fig 31 Step length versus track stiffness The solid line shows the theoretical prediction of (Eq 21) The shaded region (also shown in Fig 25) indicates the band of track stiffness where speed enhancement should be greatest (From McMahon and Greene 1979)

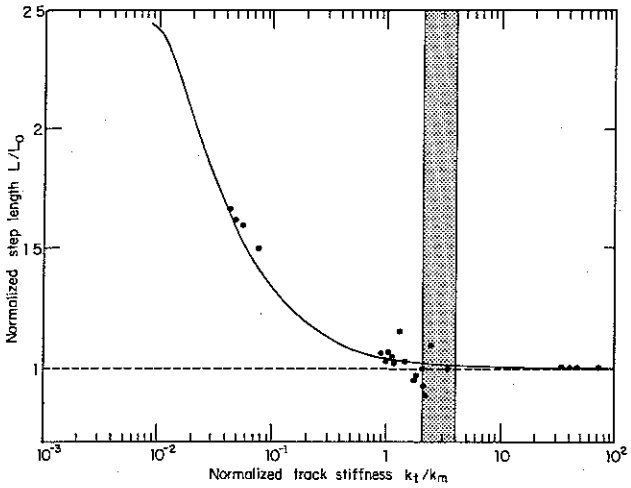

Fig 32 Tuned track at Harvard University This is a six-lane, 220-yd track with banked turns The top surface is polyurethane and the substructure, incorporating controlled compliance, is primarily wood Runners from both Harvard and other schools have averaged between 2% and 3% better times here, by comparison with their times on conventional tracks of identical length and top surface (From McMahon and Greene 1978)

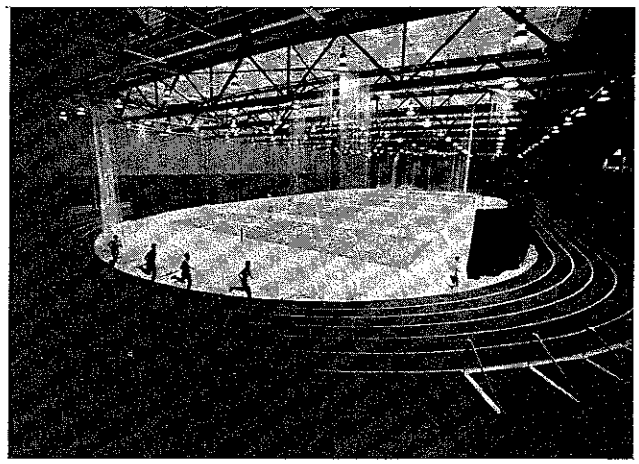

Substituting (Eq 20) into (Eq 19) with $\delta = mg/k_t$,

$$L = 2\sqrt{\ell^2 - [(\ell^2 - L_0^2/4)^{1/2} - mg/k_t]^2} \qquad (21)$$

This relation may be used to calculate L, given only the leg length ℓ, the hard-track step length L_0, the subject's mass m, and the track stiffness k_t. The solid line in Fig 31 shows this calculation, assuming $\ell = 1.09$ m and $L_0 = 0.89$ m for a 180-lb man. The points represent several runners on both the pillow track and on two separate stiffness configurations of the board track The experiments showed, in agreement with the theory, that step length is increased as track stiffness is decreased. The enhancement in step length in the tuned range (shaded) is about 1.0%

12.4. Tuned-Track Prototypes

The conclusions of the theory and experiments above are that it should be possible to build a running track within the range of spring stiffnesses shown by the shaded bands in Figs. 25 and 31 that will (1) decrease foot-contact time, (2) increase step length, and (3) reduce running injuries. The evidence for the last expectation is that the force-plate records consistently showed a large spike in foot force, often exceeding 5 times body weight, as the runner's foot struck the hard surface This spike was either absent or very much attenuated when the same subject ran on tracks of high compliance, including those in the tuned range.

In October 1977, a new 220-yd track built according to the tuned principle was placed in service at the Indoor Track and Tennis Facility at Harvard University (Fig 32) It features a substructure made of wood and synthetic materials that achieves a nearly uniform vertical compliance (i.e., without the hard and soft spots that can be a feature of wood tracks unless care is taken in the design). The top surface is a layer of solid polyurethane, which is attractive and easy to care for but does not affect compliance significantly.

The first several years of service have shown that the new track has been responsible for an abrupt reduction in the rate of running injuries—that rate is now less than half what it was on the previous training surface (cinders) Furthermore, Harvard runners and runners from other schools are able to better their times by about 2%, or about 5 s in the mile, by comparison with their times on other tracks of the same length and top surface (polyurethane).

In 1980, an 11-lap/mile portable track utilizing the same principle but including fiberglass panels in the substructure was introduced at Madison Square Garden in New York. Since its introduction, this track has acquired a reputation for being both comfortable to run on and fast. At the Milrose Games, for example, one of the most important indoor track meets in the world, new records were set in the first year in all but

one of the running events run on the new oval track, and, in many events, the first two, three, or four runners over the finish line broke previous records. In the first two seasons, seven new world records were set on the track.

No outdoor track of the optimum mechanical design has been built as of the time of writing. If such a track were to be built, the results of our research and experience with the Harvard and Madison Square Garden prototypes suggest that the world record for the mile could be bettered by 5–7 s by the best miler of that day.

References

Basmajian, J. V. 1976. *The human bicycle. Biomechanics*, vol. 5-A, ed. P. V. Komi. Baltimore: University Park Press.

Cavagna, G. A., Heglund, N. C., and Taylor, C. R. 1977. Mechanical work in terrestrial locomotion: two basic mechanisms for minimizing energy expenditure. *Am. J. Physiol.* 233(5):R243–R261.

Cavagna, G. A., Thys, H., and Zamboni, A. 1976. The sources of external work in level walking and running. *J. Physiol.* 262:639–657.

Crago, P. E., Houk, J. C., and Hasan, Z. 1976. Regulatory actions of human stretch reflex. *J. Neurophysiol.* 39:925–935.

Dawson, T. J., and Taylor, C. R. 1973. Energetic cost of locomotion in kangaroos. *Nature* 246:313–314.

Eisenberg, E., Hill, T. L., and Chen, Y. 1980. Cross-bridge model of muscle contraction. *Biophys. J.* 29:195–227.

Greene, P. R. 1983. Circle running: experiments, theory, and applications. Submitted for publication.

Grieve, D. W., and Gear, R. J. 1966. The relationships between the length of stride, step frequency, time of swing and speed of walking for children and adults. *Ergonomics* 9:379–399.

Huxley, A. F. 1957. Muscle structure and theories of contraction. *Prog. Biophys. biophys. Chem.* 7:255–318.

Inman, V. T., Ralston, H. J., and Todd, F. 1981. *Human walking*. Baltimore: Williams & Wilkins.

Kushmerick, M. J., and Paul, R. J. 1976. Relationship between initial chemical reactions and oxidative recovery metabolism for single isometric contractions of frog sartorius at 0°C. *J. Physiol.* (Lond.) 254:711–727.

Marey, E. J. 1874. *Animal mechanism. a treatise on terrestrial and aerial locomotion*. New York: Appleton.

Margaria, R. 1938. Sulla fisiologia e specialmente sul consumo energetico della marcia e della corsa a varie velocità ed inclinazioni del terreno. *Atti Accad. Naz. Lincei Memorie, serie VI*, 7:299–368.

Margaria, R. 1976. *Biomechanics and energetics of muscular exercise*. Oxford: Clarendon.

Margaria, R., and Cavagna, G. A. 1972. Biomechanics of exercise in reduced gravity. Paper delivered at 4th Man in Space Symp., Erevan, USSR.

Margaria, R., Cerretelli, P., Aghemo, P., and Sassi, G. 1963. Energy cost of running. *J. Appl. Physiol.* 18:367–370.

McMahon, T. A., and Greene, P. R. 1978. Fast running tracks. *Scientific American* 239:148–163.

McMahon, T. A., and Greene, P. R. 1979. The influence of track compliance on running. *J. Biomech.* 12:893–904.

Melvill Jones, G., and Watt, D. G. D. 1971. Observations on the control of stepping and hopping movement in man. *J. Physiol.* 219:709–727.

Mochon, S., and McMahon, T. A. 1980. Ballistic walking. *J. Biomech.* 13:49–57.

Mochon, S., and McMahon, T. A. 1981. Ballistic walking: an improved model. *Math. Biosci.* 52:241–260.

Nichols, T. R., and Houk, J. C. 1976. The improvement in linearity and the regulation of stiffness that results from actions of the stretch reflex. *J. Neurophysiol.* 39:119–142.

Sandbert, J. A., and Carlson, F. D. 1966. The length dependence of phosphorylcreatine hydrolysis during an isometric tetanus. *Biochemische Zeitschrift* 345:212–231.

Saunders, J. B., Inman, V. T., and Eberhart, H. D. 1953. The major determinants in normal and pathological gait. *J. Bone Joint Surg.* [Am.] 35A:543–558.

Stainsby, W. N., and Fales, J. T. 1973. Oxygen consumption for isometric tetanic contractions of dog skeletal muscle in situ. *Am. J. Physiol.* 224:687–691.

Taylor, C. R. 1978. Why change gaits? Recruitment of muscles and muscle fibers as a function of speed and gait. *Am. Zool.* 18:153–161.

Taylor, C. R., Heglund, N. C., McMahon, T. A., and Looney, T. R. 1980. Energetic cost of generating muscular force during running: a comparison of large and small animals. *J. Exp. Biol.* 86:9–18.

Taylor, C. R., Schmidt-Nielsen, K., and Raab, J. L. 1970. Scaling of energetic cost of running to body size in mammals. *Am. J. Physiol.* 219:1104–1107.

Taylor, C. R., Shkolnik, A., Dmi'el, R., Baharav, D., and Borut, A. 1974. Running in cheetahs, gazelles, and goats: energy cost and limb configuration. *Am. J. Physiol.* 227:848–850.

Wood, J. E. 1981. A statistical-mechanical model of the molecular dynamics of striated muscle during mechanical transients. *Lect. Appl. Math.* 19:213–259.